European Journal of Medicinal Chemistry 44 (2009) 3584–3590

Contents lists available at ScienceDirect

European Journal of Medicinal Chemistry

journal homepage: http://www.elsevier.com/locate/ejmech

Original article

Knowledge based identification of MAO-B selective inhibitors using pharmacophore and structure based virtual screening models

Kiran Boppana [a,b,*], P.K. Dubey [b], Sarma A.R.P. Jagarlapudi [a], S. Vadivelan [a], G. Rambabu [a]

[a] GVK Biosciences Pvt. Ltd., S-1, Phase-1, T.I.E., Balanagar, Hyderabad 500 037, Andhra Pradesh, India
[b] Department of Chemistry, J.N.T. University, Kukatpally, Hyderbad 500 085, Andhra Pradesh, India

ARTICLE INFO

Article history:
Received 31 December 2008
Received in revised form
23 February 2009
Accepted 27 February 2009
Available online 11 March 2009

Keywords:
MAO-B
Pharmacophore
Docking
Catalyst
Glide

ABSTRACT

Monoamine Oxidase B interaction with known ligands was investigated using combined pharmacophore and structure based modeling approach. The docking results suggested that the pharmacophore and docking models are in good agreement and are used to identify the selective MAO-B inhibitors. The best model, Hypo2 consists of three pharmacophore features, i.e., one hydrogen bond acceptor, one hydrogen bond donor and one ring aromatic. The Hypo2 model was used to screen an in-house database of 80,000 molecules and have resulted in 5500 compounds. Docking studies were performed, subsequently, on the cluster representatives of 530 hits from 5500 compounds. Based on the structural novelty and selectivity index, we have suggested 15 selective MAO-B inhibitors for further synthesis and pharmacological screening.

1. Introduction

Monoamine Oxidase (MAO) is a flavinadenosine dinucleotide containing enzyme located at the outer membranes of mitochondria in the brain, liver, intestinal mucosa, and other organs. It catalyzes the oxidative deamination of biogenic amines (neuroamines, vasoactive and exogenous amines), including dopamine, serotonin, norephinephrine, tyramine, tryptamine, and MPTP neurotoxin. The end products are aldehydes and H_2O_2 that are involved in oxidative cellular processes [1]. MAO exists in two isoforms, i.e., MAO-A and MAO-B in humans and both are 60 kDa outer-mitochondrial membrane-bound flavoenzymes that share 70% sequence identities [2]. Due to distinct and overlapping specificities of MAO-A and MAO-B in the oxidative deamination of neurotransmitters and dietary amines, the development of specific reversible inhibitors has been a long sought goal. Expression levels of MAO-B in neuronal tissue increase 4-fold with age [3], resulting in an increased level of dopamine metabolism and the production of higher levels of hydrogen peroxide, which are thought to play a role in the etiology of neurodegenerative diseases such as Parkinson's and Alzheimer's diseases [4]. MAO inhibitors demonstrated remarkable antidepressant action but their clinical value was seriously compromised with side effects like "cheese reaction" [5]. These serious side effects stimulated a search for antidepressants that are not MAO inhibitors and to their eventual replacement using the uptake inhibitors, the tricyclic antidepressants and more recently the serotonin selective re-uptake inhibitors (Prozac). Despite the general lack of interest, Knoll & Magyar persisted in their study with an irreversible MAO inhibitor, l-Deprenyl, derived from propargylamine [6,7]. It is a selective MAO-B inhibitor at low doses and inhibited the oxidative deamination of dopamine, phenylethylamine and benzylamine but at higher doses the selectivity of the compound was lost. The compound also was evaluated as an antidepressant, devoid of the "cheese reaction" [7]. Thus, the development of specific, reversible MAO-B inhibitors could lead to clinically useful neuroprotective agents. Compounds with similar structural motifs can lead to the same biological effect. It is also well accepted that bioactive ligands that bind to a common receptor must fulfill certain chemical and geometric criteria. For this purpose a knowledge-based approach is based on another popular technique applied in the drug discovery, known as scaffold-hopping [8,9] where the goal is to 'jump' in chemistry space, i.e., to discover a new structure starting from a known active compound via the modification of the central core of this molecule [10]. In the previous studies pharmacophore model was generated with the consideration of Thiazole derivatives and

* Corresponding author. GVK Biosciences Pvt. Ltd., S-1, Phase-1, T.I.E., Balanagar, Hyderabad 500037, Andhra Pradesh, India. Tel.: +91 40 23721001; fax: +91 40 23721010.
E-mail address: kiran@gvkbio.com (K. Boppana).

0223-5234/$ – see front matter © 2009 Elsevier Masson SAS. All rights reserved.
doi:10.1016/j.ejmech.2009.02.031

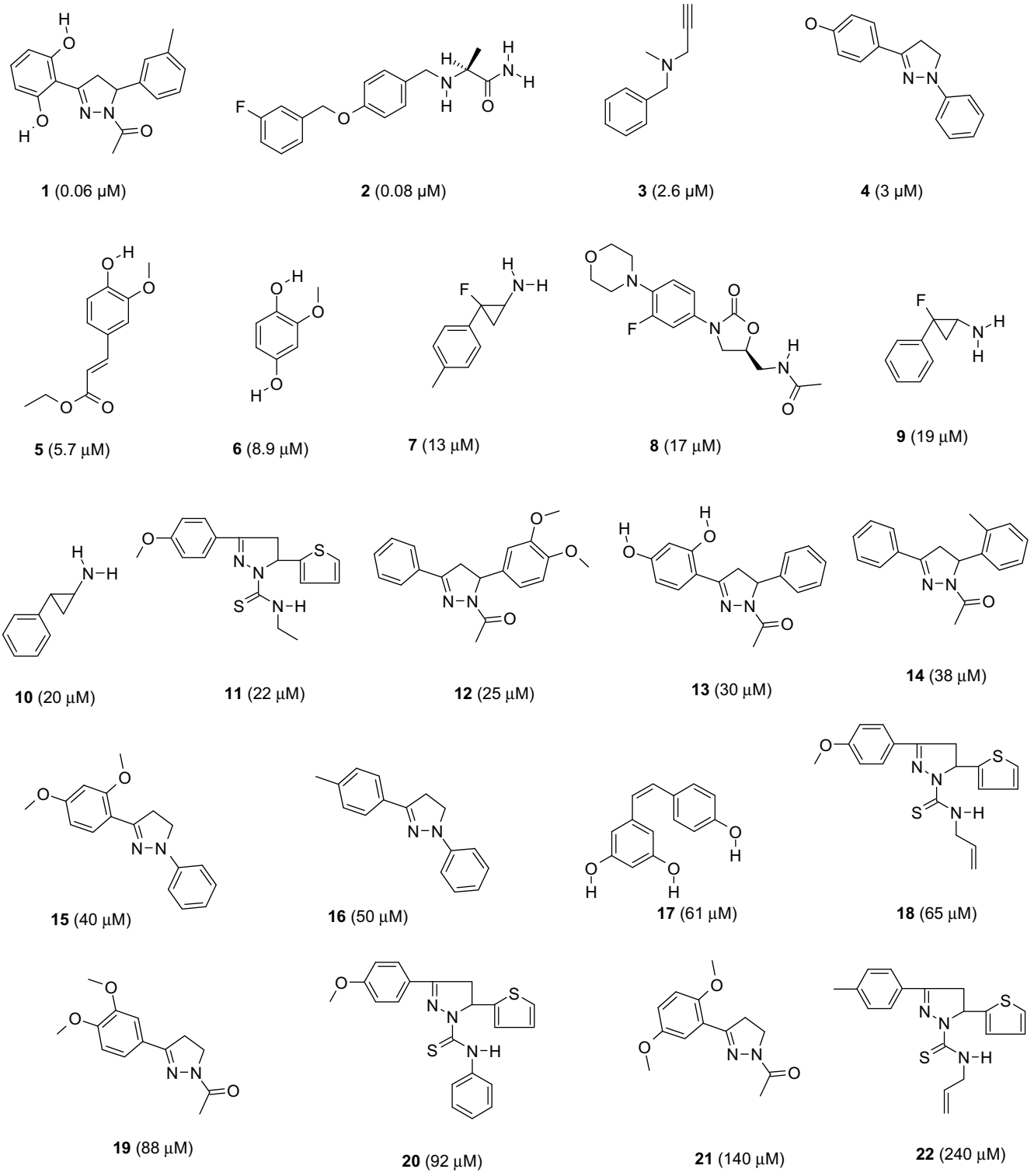

Fig. 1. Training set molecules for MAO-B inhibitors. IC50 values of each molecule are given in parentheses.

Thiosemicarbazide derivatives with features like three hydrogen bond acceptors, one hydrophobic feature and one aromatic ring [11]. In the present study, the ligand and structure based design studies were done using Catalyst and Glide to design selective MAO-B inhibitors [12–15]. We have considered diverse set of structural motifs like Thio- and semicarbazides, beta-Carbolines, *cis*- and *trans*-resveratrol derivatives, Eugenol derivatives, Pyrazoles, Oxazolidinones, Phenylcyclopropylamines, and Indan derivatives to describe the knowledge-based design, identification and optimization of a new lead [16–25]. Most of the rationally designed and clinically useful inhibitors (revesible or irreversible) are competitive inhibitors. We have included both reversible and irreversible inhibitors in the training set to get the optimized features necessary for the enzyme inhibition.

Table 1
Experimental and Predicted IC_{50} data of 22 training set molecules against Hypo2 model.

Molecule	Experimental IC_{50}, μM	Predicted IC_{50}, μM	Error[a]	Fit value[b]	Experimental scale[c]	Predicted scale[c]
1	0.06	0.114	2.4	4.81	+++	+++
2	0.08	0.11	2.6	5.41	+++	+++
3	2.6	7.2	5.9	3.54	+++	+++
4	3	11.2	6.8	3.41	+++	+++
5	6.7	9.8	1.5	3.73	+++	+++
6	8.9	19	2.7	3.34	+++	+++
7	13	14	1.1	3.57	+++	+++
8	17	8.2	−6	4.27	+++	+++
9	19	14	−1.3	3.57	+++	+++
10	20	13	−1.6	3.62	++	+++
11	22	24	1.1	3.35	++	++
12	25	21	−1.2	3.4	++	++
13	30	25	−1.2	3.32	++	++
14	38	21	−1.8	3.41	++	++
15	40	35	−2	3.43	++	++
16	50	21	−2.4	3.41	++	++
17	61	38	−1.6	3.14	+	++
18	65	34	−1.9	3.2	+	++
19	88	190	2.15	2.26	+	+
20	92	39	−2.4	3.14	+	++
21	140	210	1.5	2.24	+	+
22	240	148	−5	3.05	+	+

[a] + Indicates that the Predicted IC_{50} is higher than the Experimental IC_{50}; − indicates that the Predicted IC_{50} is lower than the Experimental IC_{50}; a value of 1 indicates that the predicted IC_{50} is equal to the Experimental IC_{50}.
[b] Fit value indicates how well the features in the Pharmacophore overlap the chemical features in the molecule. Fit = weight*[max(0,1−SSE)] where SSE = (D/T)2, D = displacement of the feature from the center of the location constraint and T = the radius of the location constraint sphere for the feature (tolerance).
[c] Activity scale − IC_{50} <20 μM = +++ (Highly active) − IC_{50} 20–50 μM = ++ (Moderately active) − IC_{50} >50 μM = + (Low active).

Table 2
10 Pharmacophore models generated by the HypoGen for MAO-B inhibitors.

Hypo no.	Total cost	Cost difference[a]	Error cost	RMS deviation	Training set (*r*)	Features[b]
1	100.46	55.42	83.92	0.941	0.772	HBA,HBD,RA
2	**99.04**	**56.84**	**82.42**	**0.875**	**0.961**	**HBA,HBD,RA**
3	99.58	56.3	82.8	0.894	0.892	HBA,HBD,RA
4	99.64	56.24	82.87	0.898	0.851	HBA,HBD,RA
5	100.06	55.82	83.23	0.916	0.812	HBA,HBD,RA
6	100.11	55.77	83.54	0.931	0.783	HBA,HBD,RA
7	100.77	55.11	84.11	0.958	0.769	HBA,HBD,RA
8	100.99	54.89	83.45	0.927	0.79	HBA,HBD,RA
9	101.12	54.76	84.36	0.97	0.763	HBA,HBD,RA
10	101.19	54.69	83.35	0.922	0.793	HBA,HBD,RA

Hypo 2 showed a better correlation coefficient (0.945) compared to the other nine hypotheses.
[a] (Null cost−Total cost), Null cost = 155.88, Fixed cost = 90.53, For the Hypo-2 Weight = 1.28, Configuration = 15.41. All cost units are in bits.
[b] HBA – Hydrogen Bond Acceptor, HBD – Hydrogen bond donor, RA – Ring aromatic.

2. Results and discussion

2.1. Pharmacophore generation and validation studies

The best common feature pharmacophore model [19] indicated the importance of H-bond acceptor (HBA), H-bond donor (HBD) and ring aromatic (RA) features, which were further confirmed in the quantitative models. Several quantitative models were generated utilizing the training set (**1**–**22**) along with MAO-B inhibitory activities (Fig. 1 and Table 1). The top ten hypotheses were composed of HBA, HBD, and RA features. The values of ten hypotheses such as cost, correlation (r), and root-mean-square deviations (rmsd) are statistically significant (Table 2). It is evident that as error, weight and configuration components are very low and not deterministic to the model, the total pharmacophore cost is

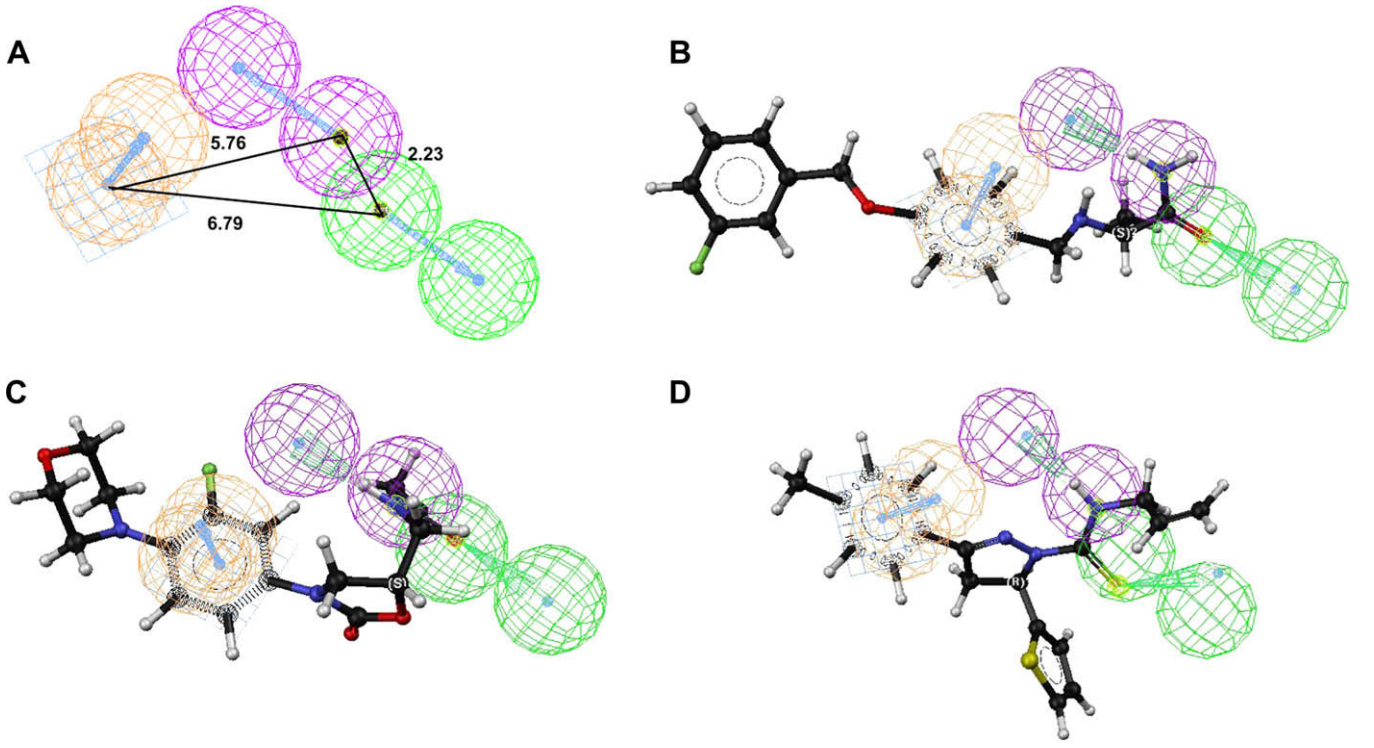

Fig. 2. Pharmacophore model for MAO-B inhibitors. (A) Three-dimensional arrangement of pharmacophore features in the quantitative pharmacophore model (Hypo2). Pharmacophore features are: H-bond acceptor (HBA) as green, Ring aromatic (RA1) as orange and H-bond donor (HBD) as magenta. (B) Hypo2 is mapped onto high active compound (**2**). (C) Mapping of Hypo2 onto a moderately active compound 8. (D) Mapping of Hypo2 onto an inactive compound **22**. (For interpretation of the references to colour in this figure legend, the reader is referred to the web version of this article.)

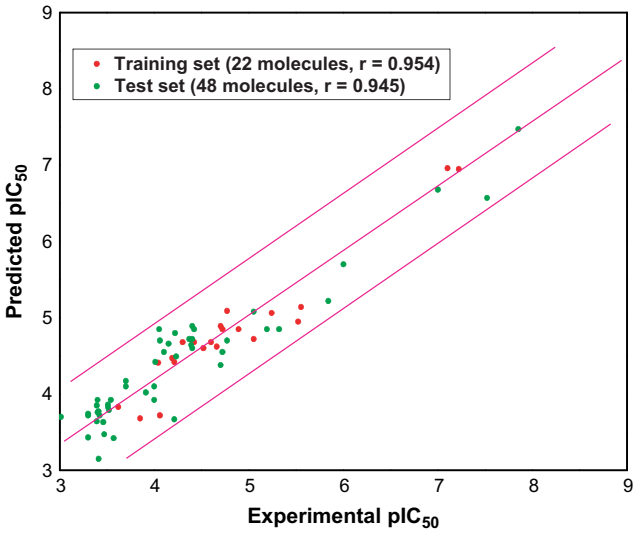

Fig. 3. Scatter plot shows correlation between experimental and Hypo2 predicted activities of known MAO-B inhibitors.

also low and close to the fixed cost. Also, as total cost is less than the null cost, this model accounts for all the pharmacophore features and has good predictive ability. In addition to an estimation of activity of the training set molecules, the pharmacophore model should also accurately predict the activity of the test set molecules. Two statistical methods were employed to rank the ten resultant

Table 3
Statistical parameters from screening of training and test set molecules.

Serial No	Parameter	MAO-B
1	Total molecules in database (D)	70
2	Total number of actives in database (A)	34
3	Total hits (Ht)	38
4	Active hits (Ha)	32
5	% Yield of actives [(Ha/Ht)*100]	84.21
6	% Ratio of actives [(Ha/A)*100]	94.12
7	Enrichment factor (E) [(Ha*D)/(Ht*A)]	1.76
8	False negatives [A−Ha]	2
9	False positives [Ht−Ha]	6
10	Goodness of hit score[a]	0.73

[a] [(Ha/4HtA)(3A + Ht))*(1−((Ht−Ha)/(D−A))]; GH Score of 0.7–0.8 indicates a very good model.

hypotheses. In the first method, all ten hypotheses were evaluated using a test set of 48 known MAO-B inhibitors, which are not included in the training set. Predicted activities of the test set were calculated using all ten hypotheses and correlated with experimental activities. Of the ten hypotheses, Hypo2 showed a better correlation coefficient (0.945) compared to the other nine hypotheses. A second statistical test includes calculation of false positives, false negatives, enrichment, and goodness of hit to determine robustness of hypotheses. Under all validation conditions, Hypo2 performed superior as compared to the other nine hypotheses. Hypo2 demonstrated excellent prediction of MAO-B inhibitory activities of the training set compounds (Table 1). Analyzing the results, it was observed that out of the 9 highly active molecules, all were predicted correctly as highly active. Among the

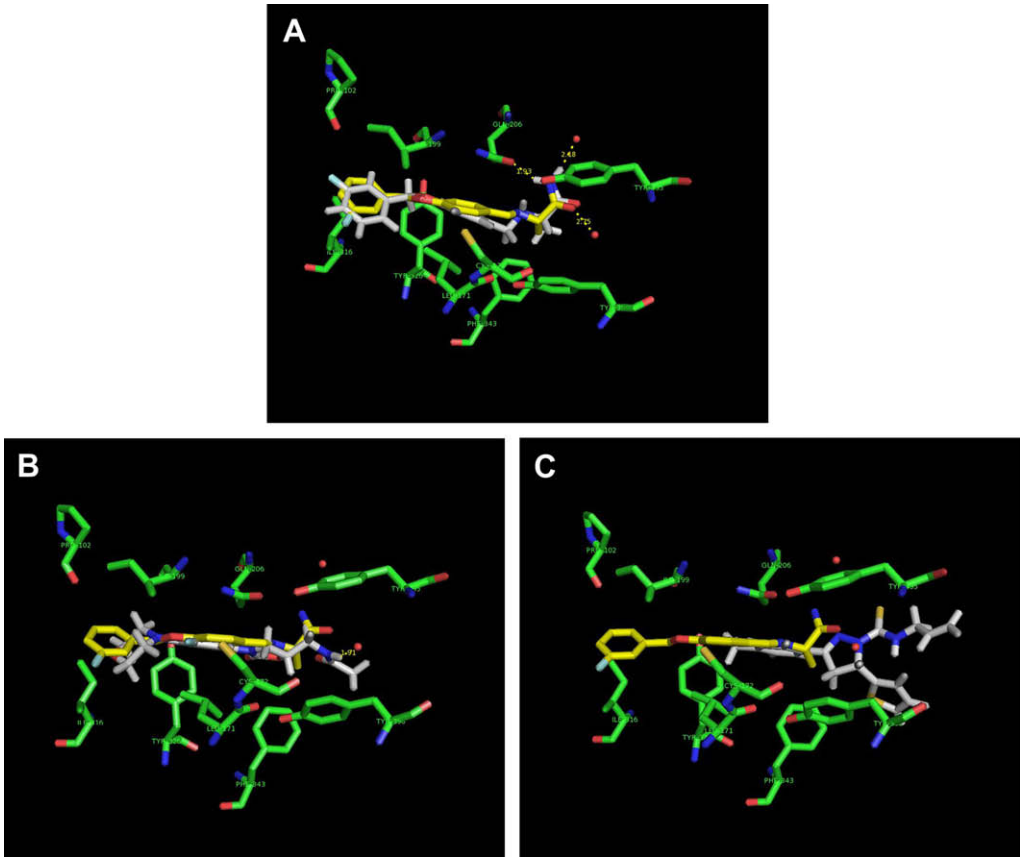

Fig. 4. GLIDE docking studies on MAO-B inhibitors. (A) The bound conformation of compounds 2 (white) and Crystal ligand (yellow) on the Active Site of MAO-B. (B) The bound conformation of compounds 8 (white) and Crystal ligand (yellow) on the Active Site of MAO-B. (C) The bound conformation of compounds 22 (white) and Crystal ligand (yellow) on the Active Site of MAO-B. (For interpretation of the references to colour in this figure legend, the reader is referred to the web version of this article.)

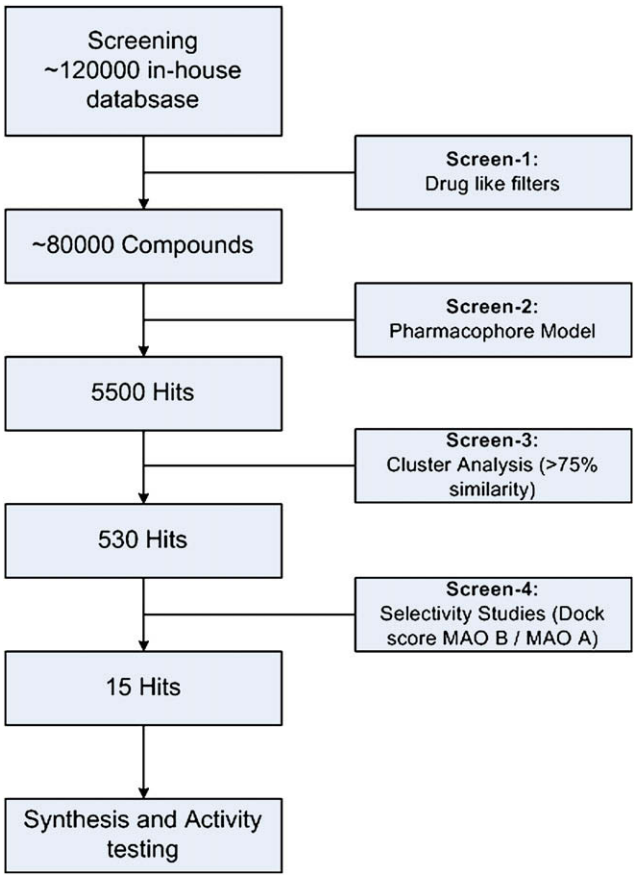

Fig. 5. Schematic representation of in silico screening protocol implemented in the identification of MAO-B inhibitors.

6 moderately active molecules, except one, which was predicted as highly active and the rest were correctly predicted. Out of the 6 low active molecules, 3 were predicted as moderately active and the rest was predicted as low active. Activities of the compounds were not only correctly predicted but also the fit values confer a good measure of how well the pharmacophoric features of Hypo2 were mapped onto the chemical features of the compounds. Fig. 2A shows the HypoGen pharmacophore features with their geometric parameters, all features of Hypo2 (HBA, HBD and RA) were mapped onto the highly active compounds of the training set (**2**) as well as the moderate compound (**8**) shown in Fig. 2B and C respectively. Many of the low active compounds in the training set (**22**) were mapped partially by the features of Hypo2 (Fig. 2D).

The correlation values along with the predictions above make the pharmacophore suitable to predict molecular properties well. The plot showing the correlation between the actual and predicted activities for the test set and the training set molecules is given in Fig. 3.

The purpose of the pharmacophore model generation is not just to predict the activity of the training set compounds accurately but also to verify whether the pharmacophore models are capable of predicting the activities of external compounds of the test set series and classifying them correctly as active or inactive. The molecules were classified as highly active (+++ or $<$20 μM), moderately active (++ or 20–50 μM) and inactive (+ or $>$50 μM). Hypo2 was used to search the test set of known MAO-B inhibitors. Database mining was performed using the BEST flexible searching technique. The results were analyzed using a set of parameters such as hit list (Ht), number of active percent of yields (%Y), percent ratio of actives in the hit list (%A), enrichment factor (E), false negatives, false positives, and goodness of hit score (GH) (Table 3) [31]. Hypo2 succeeded in the retrieval of 84% of the active compounds. In addition, the pharmacophore also retrieved 6 inactive compounds (false positives) and predicted 2 active compounds as inactive (false negatives). An enrichment factor of 1.76 and a GH score of 0.73 indicate the quality of the model. Overall, a strong correlation was observed between the Hypo2 predicted activity and the experimental MAO-B inhibitory activity (IC_{50}) of the training and test set compounds (Fig. 3). However, the Hypo2 model has a greater tendency to show false positives. This could be attributed to high structural similarity in active and inactive MAO-B inhibitors, resulting in an inability to discriminate this pattern by the pharmacophore model. We further extended this study to structure-based design and to limit the number of false positive and false negative hits and to further understand the binding of inhibitors to the active site of MAO-B complex.

2.2. GLIDE docking studies

A set of 70 MAO-B inhibitors were docked onto MAO-B active site using Glide in order to identify their binding sites. A general trend was observed, in which the more active compound complexes scored higher than moderate active and low active compounds. Overall, there was no significant correlation between the fitness scores and MAO-B inhibitory activities of the compounds. Fig. 4 depicts a comparison between the bound conformation of representative highly active (**2**), moderately active (**8**) and low active (**22**) compounds inside the active site of MAO-B. The predicted binding areas of highly active compound and moderate in the MAO-B active site were similar to that of crystal ligand (Fig. 4A and B). Hydrogen bonding interactions and the interacting amino acid residues at the active site are also shown in Fig. 2. These compounds commonly occupy a wide cavity surrounded by the following amino acids: Y60, P102, L171, I198, I199, Q206, I316, Y326, F343, Y398, and Y435. It was observed that the active compound established strong interactions with key amino acid residues and the amide nitrogen of highly active is engaged in two hydrogen bonds with Gln206 and an ordered water molecule and the amide oxygen is H-bonded to a water molecule. In the moderate active compound only one hydrogen bond formation was observed with water molecule where in low active compound neither showing any hydrogen bonding nor occupying the crystal ligand active site place. This analysis concludes the impartment interaction between the MAO-B protein and ligand and also correlated these interactions with pharmacophore features.

2.3. Compound selection

The compound selection process implemented is shown as a flowchart in Fig. 5. The pharmacophore model (Hypo2) was used as a query to screen an in house database consisting of 80,000 compounds which were passed drug like filters. The search retrieved 5500 compounds were selected for cluster analysis and a set of 530 cluster representative hits with predicted IC_{50} value of less than 10 μM were chosen for docking onto the active site of MAO-B. Highly scored compounds were selected to carry out the docking analysis onto the active site of MAO-A. Finally, 15 hits (Fig. 6) were chosen for synthesis and testing based on selectivity index (MAO-B Glide Score/MAO-A Glide Score $>$1) of the compounds, structural novelty and feasibility of synthesis. Detailed synthetic process and activity profile of these compounds are in progress in our laboratory and will be presented in due course.

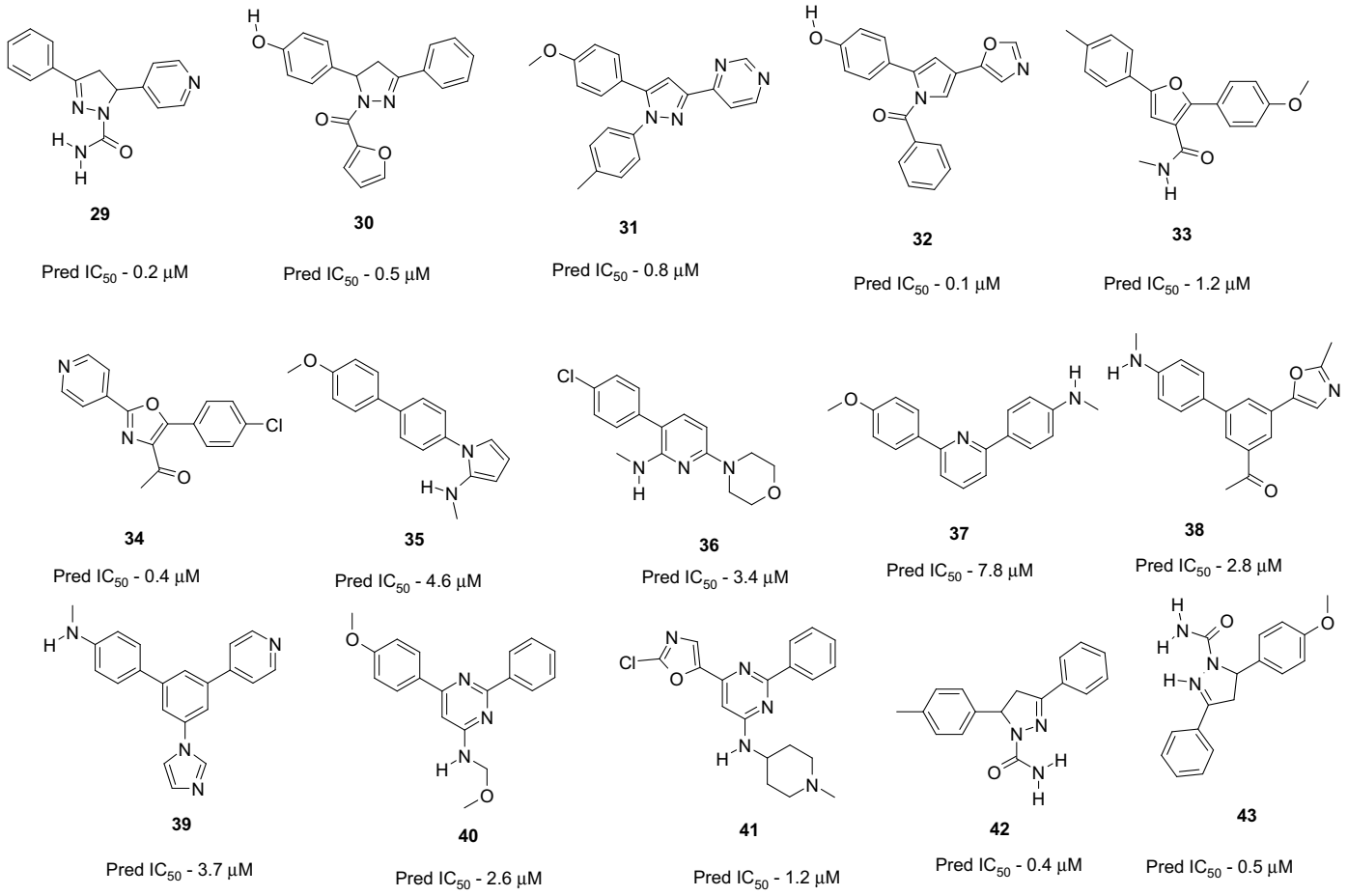

Fig. 6. Structurally diverse set of compounds retrieved from the database and proposed for synthesis.

3. Conclusion

Several structurally diverse compounds possessing MAO-B selective inhibitory activity were identified using pharmacophore and docking studies. These compounds bearing amenable chemical and structural features are potential leads for drug design strategies targeting MAO-B. Further compound synthesis and their inhibitory activity will be reported in due course.

4. Materials and methods

4.1. Pharmacophore model generation and validation

Pharmacophore modeling correlates activities with the spatial arrangement of various chemical features in a set of active analogues. A set of 70 human MAO-B inhibitors [16–25] with an activity range (IC_{50}) spanning over 5 orders of magnitude, i.e., 0.014–980 μM were selected. Molecules were chosen based on the MAO-B inhibitory assay tested under similar experimental conditions. This initial group was then divided into the training and test sets. The training set of 22 molecules was designed to be structurally diverse with a wide activity range. The training set molecules play a critical role in the pharmacophore generation process and the quality of the resultant pharmacophore models relies solely on the training set molecules. The test set of remaining 48 molecules is designed to evaluate predictive ability of the resultant pharmacophore. Highly active (+++ or <20 μM), moderately active (++ or 20–50 μM) and inactive (+ or >50 μM) compounds were added to the training set to obtain critical information on pharmacophore requirements for MAO-B inhibition. The molecules selected as the training set are given in Fig. 1. This training set was then used to generate quantitative pharmacophore models.

Qualitative pharmacophore models were generated using a set of highly active molecules. To confirm essential features prevailing among the MAO-B inhibitors, 10 common feature hypotheses were generated using the most active molecules 1–6 (Fig. 1). The common features for all 10 hypotheses are hydrogen bond donor, hydrogen bond acceptor and ring aromatic features. However, these models cannot be directly used to predict biological activity of the compounds retrieved from a database. We have generated quantitative pharmacophore models to predict the biological activities of novel compounds. While generating the quantitative model, a minimum of 0 to a maximum of 5 features involving HBA, HBD, and RA features were selected and used to build a series of hypotheses using a default uncertainty value of 3. The quality of HypoGen models are best described by Debnath and Vadivelan [26–29] in terms of Fixed Cost, Null Cost and total Cost and other statistical parameters. According to which, a large difference between the fixed cost and null cost, and a value of 40–60 bits for the unit of cost would imply 75–90% probability for experimental and predicted activity correlation. In general, pharmacophore models should be statistically significant, predict the activity of molecules accurately, and retrieve active compounds from a database. The derived pharmacophore models were validated using a set of parameters including cost analysis, test set prediction, enrichment factor, and goodness of hit. HipHop and HypoGen

modules within Catalyst were then used to generate qualitative pharmacophore and quantitative pharmacophore models, respectively.

4.2. GLIDE docking studies

Crystal structure of MAO-A (PDB code: 2BXR) and MAO-B (PDB code: 2V5Z) [25] were used for the docking studies [30]. The protein 3D structures were downloaded from the protein databank (PDB). The hydrogen atoms were added to the proteins and further minimization was performed using protein preparation wizard. A set of 70 human MAO-B inhibitors were docked on to the active site of MAO-A and MAO-B using Glide docking program. During the docking process, Glide initially performs a complete systematic search of the conformation, orientation, and position of a compound in the defined binding site and eliminates unwanted poses using scoring and energy optimization. Finally the conformations were further refined via a Monte Carlo sampling. The MAO-A and MAO-B grid boxes were defined by the center of the bound inhibitors of the MAO-A and MAO-B proteins respectively. The enclosing box and binding box dimensions were fixed to 14 and 10 Å, respectively. The top 20 poses were collected for each compound. Docking poses were energy minimized using the OPLS-2001 force field. The best pose was selected based on Glide score and the favorable interactions formed between the compound and amino acid residues of the MAO-A and MAO-B active site. The selectivity index of the compound was calculated using the Glide score of MAO-A and MAO-B (MAO-B Glide score/MAO-A Glide score >1).

Acknowledgements

Kiran would like to thank D.S. Brar, Chairman, G.V. Sanjay Reddy, MD and Manni Kantipudi, President of GVK Biosciences Pvt. Ltd., for their continuous support and encouragement.

References

[1] J.P. Johnson, Biochem. Pharmacol. 17 (1968) 1285–1297.
[2] J.C. Shih, K. Chen, M.J. Ridd, Annu. Rev. Neurosci. 22 (1999) 197–217.
[3] J.S. Fowler, J. Logan, G.J. Wang, N.D. Volkow, F. Telang, W. Zhu, D. Francheschi, N. Pappas, R. Ferrieri, C. Shea, V. Garza, Y. Xu, D. Schlyer, S.J. Gately, Y.S. Ding, D. Alexhoff, D. Warner, N. Netusil, P. Carter, M. Jayne, P. King, P. Vaska, Proc. Natl. Acad. Sci. U.S.A. 100 (2003) 11600–11605.
[4] M.J. Kumar, D.G. Nicholls, J.K. Andersen, J. Biol. Chem. 278 (2003) 46432–46439.
[5] U. Trendelenburg, N. Weiner, Monoamine Oxidase, in: M.B.H. Youdim, J.P.M. Finberg, K.F. Tipton (Eds.), Advances in Experimental Pharmacology, Springer-Verlag, Berlin, 1988, pp. 119–192.
[6] J. Knoll, K. Magyar, Adv. Biochem. Psychopharmacol. 5 (1972) 393–408.
[7] Moussa B.H. Youdim, Y.S. Bakhle, Br. J. Pharmacol. 147 (2006) S287–S296.
[8] H.J. Bohm, A. Flohr, M. Stahl, Drug Discov. Today Technol. 1 (2004) 217–224.
[9] H. Zhao, Drug Discov. Today 12 (2007) 149–155.
[10] P. Ertl, S. Jelfs, J. Muhlbacher, A. Schuffenhauer, P. Selzer, J. Med. Chem. 49 (2006) 4568–4573.
[11] S. Gritsch, S. Guccione, R. Hoffmann, A. Cambria, G. Raciti, T. Langer, J. Enzyme Inhib. 16 (2001) 199–215.
[12] Maestro, Version 1.0.9113, Schrodinger, L.L.C., New York, 2006.
[13] Glide, Version 3.5, Schrodinger, L.L.C., New York, 2006.
[14] Cerius^2, Version 4.11, Accelrys Inc., San Diego, CA 92121, USA, 2007.
[15] Catalyst, Version 4.11, Accelrys Inc., San Diego, CA 92121, USA, 2007.
[16] G. Nesrin, Y.S. Akgul, U. Gulberk, E. Kevser, A.B. Altan Bilgina, Arch. Pharm. Pharm. Med. Chem. 336 (2003) 362–371.
[17] T. Herraiz, C. Chaparro, Biochem. Biophys. Res. Commun. 326 (2005) 378–386.
[18] M. Yanez, N. Fraiz, E. Cano, F. Orallo, Biochem. Biophys. Res. Commun. 344 (2006) 688–695.
[19] T. Guoxin, I. Yoshifumi, L. Dian-Jun, M.K. Wing, Bioorg. Med. Chem. 13 (2005) 4777–4788.
[20] F. Chimenti, A. Bolasco, F. Manna, D. Secci, P. Chimenti, A. Granese, O. Befani, P. Turini, S. Alcaro, F. Ortuso, Chem. Biol. Drug Des. 67 (2006) 206–214.
[21] D.K. Hutchinson, Curr. Top. Med. Chem. 3 (2003) 1021–1042.
[22] T.C. Rosen, S. Yoshida, R. Fröhlich, K.L. Kirk, G. Haufe, J. Med. Chem. 47 (2004) 5860–5871.
[23] F. Hubálek, C. Binda, M. Li, Y. Herzig, J. Sterling, M.B. Youdim, A. Mattevi, D.E. Edmondson, J. Med. Chem. 47 (2004) 1760–1766.
[24] E.Y. Wang, H. Gao, L. Salter-Cid, J. Zhang, L. Huang, E.M. Podar, A. Miller, J. Zhao, A. O'rourke, M.D. Linnik, J. Med. Chem. 49 (2004) 2166–2173.
[25] C. Binda, J. Wang, L. Pisani, C. Caccia, A. Carotti, P. Salvati, D.E. Edmondson, A. Mattevi, J. Med. Chem. 50 (2004) 5848–5852.
[26] A.K. Debnath, J. Med. Chem. 45 (2002) 41–53.
[27] S. Vadivelan, B.N. Sinha, I. Sheeba Jem, J.A.R.P. Sarma, J. Chem. Inf. Model. 47 (2007) 1526–1535.
[28] S. Vadivelan, B.N. Sinha, G. Rambabu, B. Kiran, J.A.R.P. Sarma, J. Mol. Graph Model. 26 (2008) 935–946.
[29] S. Vadivelan, B.N. Sinha, T. Sunita, J.A.R.P. Sarma, Eur. J. Med. Chem. in press., doi:10.1016/j.ejmech.2008.08.012
[30] H.M. Berman, J. Westbrook, Z. Feng, G. Gilliland, T.N. Bhat, H. Weissig, I.N. Shindyalov, P.E. Bourne, Nucleic Acids Res. 28 (2000) 235–242.
[31] O.F. Guner, D.R. Henry, in: Osman F. Guner (Ed.), Phamacophore Perception, Development, and Use in Drug Design, International University Line, La Jolla, California, 2000, pp. 193–210.